Iron(III) Porphyrin-Imidazole Complexes. Analysis of Carbon-13 Nuclear Magnetic Resonance Isotropic Shifts and Unpaired Spin Delocalization

Harold M. Goff

Contribution from the Department of Chemistry, University of Iowa, Iowa City, Iowa 52242.
Received August 12, 1980

Abstract: Low-spin iron(III) porphyrin complexes with variously substituted imidazoles have been investigated in detail by carbon-13 NMR spectroscopy. Porphyrin structural types examined include tetraphenylporphyrins, octaalkylporphyrins, and natural-derivative porphyrins. From an empirical standpoint the carbon-13 spectra should facilitate location and assignment of hemoprotein resonances and provide strategy for biosynthetic or chemical incorporation of carbon-13 labels. Bis-ligated cobalt(III) analogues were employed as diamagnetic reference compounds. Measurement of axial ligand dynamics and magnetic anisotropy yielded values equivalent to those previously reported from proton NMR spectral studies. Variable-temperature measurements revealed only approximate Curie law behavior with generally downfield intercepts at the high-temperature limit. Separation of metal-centered dipolar shift values was made possible by the fact that phenyl carbon atoms of the tetraphenylporphyrin complexes exhibit predominantly an upfield metal-centered dipolar shift. Combined treatment of carbon-13 and proton isotropic shift data by the Karplus and Fraenkel relationships permitted separation of the ligand-centered dipolar term, dissection of the contact term into various contributions, and estimation of spin densities at porphyrin carbon and nitrogen atoms. The upfield ligand-centered dipolar contribution of −66 ppm per 1% unpaired spin density is of the same magnitude as the contact term. Estimated spin density values are: β-pyrrole carbon, +0.012; α-pyrrole carbon, +0.0055; meso carbon, −0.0015; and pyrrole nitrogen, +0.010. The approach employed here remains to be evaluated by other physical methods, upgraded theoretical calculations, and application to other metalloporphyrins.

Introduction

The imidazole moiety of histidine is apparently involved as a strong-field ligand in at least one functional form of all hemoproteins. The ligand generally occupies an axial position trans to coordinated substrate or a second amino acid residue. Two axial imidazole groups are utilized in class-*b* cytochromes.[1] Thus, the bis-ligated, low-spin iron(III) porphyrin complexes generated upon addition of imidazole to solutions of isolated iron porphyrins properly serve as cytochrome *b* active site analogues, although the species are often invoked as models for low-spin hemoproteins in general.[2-6]

An impressive number of physical-chemical techniques have been applied toward elucidation of bonding and reaction mechanisms in model iron(III) porphyrin-imidazole complexes.[7,8] Proton NMR spectroscopy has proven invaluable in determination of ligand exchange dynamics and thermodynamics,[9,10] unpaired spin delocalization,[2,3,11] and solution magnetic anisotropy.[2,11] Preliminary results of complementary carbon-13 NMR measurements have been reported from this laboratory.[5] Rationales for examination of an additional nucleus are to be found in the potential application of carbon-13 NMR to hemoproteins[12] and evaluation of earlier proton NMR analysis of unpaired spin delocalization mechanisms.[11] Carbon-13 NMR exhibits advantages of larger dispersion and more narrow line widths, but low sensitivity necessitates chemical or biological incorporation of carbon-13 labels in hemoproteins. Reason dictates examination of model iron porphyrin complexes (at normal isotopic abundance) prior to initiation of heroic labeling experiments. Model work provides strategy for such label incorporation and should facilitate location and assignment of hemoprotein signals.

Natural-abundance carbon-13 spectra of free-base porphyrins[13-15] and diamagentic metalloporphyrins[14-19] have been recorded in numerous studies. Carbon-13 spectra of the paramagnetic low-spin iron(III) porphyrin-cyanide complexes have also been reported by three research groups.[15-17,20] In their earlier study Wüthrich and Bauman[16] attempted to separate relative contributions to the isotropic (paramagnetic) shifts via theory originally developed for electron spin resonance spectroscopy of organic radicals.[21] Although it will be shown that conclusions are in agreement with our own, inability to separate the metal-centered dipolar term in the earlier work left considerable uncertainty in the results. Horrocks and Greenberg have demonstrated that imidazole ligation to iron(III) porphyrins yields considerably smaller second-order Zeeman contributions than does cyanide ligation.[22] Thus, separation of the carbon-13 metal-centered dipolar term for bis(imidazole) complexes has proven possible by methods devised for proton NMR spectroscopy.

(1) Moore, G. R.; Williams, R. J. P. *Coord. Chem. Rev.* **1976**, *18*, 125-197.
(2) La Mar, G. N.; Walker, F. A. *J. Am. Chem. Soc.* **1973**, *95*, 1782-1790.
(3) Satterlee, J. D.; La Mar, G. N. *J. Am. Chem. Soc.* **1976**, *98*, 2804-2808.
(4) Goldammer, E. v.; Zorn, H. *Mol. Phys.* **1976**, *32*, 1423-1435.
(5) Goff, H. *J. Chem. Soc., Chem. Commun.* **1978**, 777-778.
(6) Goldammer, E. v. *Z. Naturforsch., C* **1979**, *34*, 1106-1111.
(7) "Porphyrins and Metalloporphyrins"; Smith, K. M., Ed.; Elsevier: Amsterdam, 1975.
(8) "The Porphyrins"; Dolphin, D., Ed.; Academic Press: New York, 1978; Vol III-V.
(9) Satterlee, J. D.; La Mar, G. N; Frye, J. S. *J. Am. Chem. Soc.* **1976**, *98*, 7275-7282.
(10) Satterlee, J. D.; La Mar, G. N.; Bold, T. J. *J. Am. Chem. Soc.* **1977**, *99*, 1088-1093.
(11) (a) La Mar, G. N.; Walker, F. A. In ref 8, Vol IV, Chapter 2. (b) La Mar, G.N. In "Biological Applications of Magnetic Resonance"; Shulman, R.G., Ed.; Academic Press: New York, 1979; pp 305-343.
(12) Morrow, J.S.; Gurd, F.R.N. *C. R. C. Crit. Rev. Biochem.* **1975**, *3*, 221-287.
(13) (a) Doddrell, D.; Caughey, W.S. *J. Am. Chem. Soc.* **1972**, *94*, 2510-2512. (b) Matwiyoff, N.A.; Burnham, B.F. *Ann. N.Y. Acad. Sci.* **1973**, *206*, 365-382.
(14) (a) Abraham, R.J.; Hawkes, G.E.; Smith, K.M. *J. Chem. Soc., Perkin Trans. 2*, 1974, 627-634. (b) Abraham, R.J.; Hawkes, G.E.; Hudson, M.F.; Smith, K.M. *Ibid.* **1975**, 204-211.
(15) Goff, H.; Morgan, L.O *Bioinorg. Chem.* **1978**, *9*, 61-79.
(16) Wüthrich, K.; Baumann, R. *Helv. Chim. Acta* **1973**, *56*, 585-596.
(17) Wüthrich, K.; Baumann, R. *Helv. Chim. Acta* **1974**, *57*, 336-350.
(18) Eaton, S.S.; Eaton, G.R *Inorg. Chem.* **1976**, *15*, 134-139.
(19) (a) Abraham, R.J.; Pearson, H.; Smith, K.M. *J. Am. Chem. Soc.* **1976**, *98*, 1604-1606. (b) Abraham, R.J.; Eivazi, F.; Pearson, H.; Smith, K.M. *Tetrahedron* **1977**, *33*, 2277-2285. (c) Abraham, R.J.; Fell, S.C.M.; Pearson, H.; Smith, K.M. *Tetrahedron* **1979**, *35*, 1759-1766.
(20) La Mar, G.N.; Viscio, D.B.; Smith, K.M.; Caughey, W.S.; Smith, M.L. *J. Am. Chem. Soc.* **1978**, *100*, 8085-8092.
(21) Karplus, M.; Fraenkel, G.K. *J. Chem. Phys.* **1961**, *35*, 1312-1323.
(22) Horrocks, W.DeW.; Greenberg, E.S. *Mol. Phys.* **1974**, *27*, 993-999.

0002-7863/81/1503-3714$01.25/0

Additional treatment of the isotropic shift values has allowed identification of detailed contributions to the carbon-13 shifts and calculation of porphyrin spin density values. Results must be considered as estimates until evaluated by appropriate theoretical treatment or other physical measurements.

Experimental Section

Iron(III) Porphyrins. Tetraphenylporphyrin, TPP(R), derivatives were prepared by literature methods based on pyrrole–benzaldehyde condensation in a propionic acid reflux.[23] Octaethylporphyrin (OEP) and etioporphyrin I (ETIO) compounds were obtained via total pyrrole synthesis.[24] Chromatographic purification by silica gel and/or alumina dry column methods followed iron insertion in a dimethylformamide reflux.[25] Conversion to the chloride complex was ensured by brief reaction with HCl gas or by stirring a methylene chloride solution of the iron porphyrin with aqueous 1 M HCl. Natural-derivative iron(III) porphyrin dimethyl ester chloride complexes were prepared by standard methods.[26] Homogeneity of products was demonstrated by thin layer chromatography on silica gel plates developed with methylene chlroide, or mixtures containing small amounts of methanol. Compounds were further characterized by visible–ultraviolet spectroscopy and proton NMR spectra of both high-spin[11] and low-spin[11] bis(imidazole)iron(III) complexes.

Cobalt(III) Porphyrins. Cobalt(II) tetraphenylporphyrins were prepared by the general technique of metal salt reaction in a dimethylformamide reflux.[25] The solid product was isolated by addition of water to the cooled dimethylformamide reaction mixture. The crude cobalt(II) porphyrin (0.25 g) was dissolved in 50 mL of chloroform to which was added 2 mL of 1-methylimidazole (1-MeIm). This solution along with 10 mL of 0.5 M aqueous NaCl was stirred vigorously at 45 °C for 2 h to promote air oxidation. The chloroform layer was washed twice with water, dried over $CaCl_2$, and reduced to 10 mL volume. This solution was applied to a 2.5 × 20 cm column of dry alumina. Chloroform elution allowed separation of metal-free porphyrin and two small green bands. The product was eluted with 5% methanol in chloroform, filtered, and evaporated to dryness under reduced pressure. Dissolution in chloroform and addition of heptane with slow evaporation afforded microcrystalline material which was separated by filtration and vacuum dried at room temperature (yield: 0.18 g). Proton (integrations) and carbon-13 NMR spectra were consistent with the expected[27-29] cobalt(III) porphyrin–bis(1-methylimidazole) structure (vide infra).

Synthesis of analogous cobalt(III) ETIO complexes by this scheme was also possible by increasing the volume of chloroform solvent to accomodate this less soluble derivative. Proton NMR integrations were consistent with bis(1-methylimidazole) ligation, although mono-base adducts are known.[30,31]

Imidazoles. Imidazole (Sigma) was repeatedly recrystallized from benzene. Other imidazole derivatives, to include 1-methylimidazole (Aldrich), 5(4)-methylimidazole (Research Organic/Inorganic Chemical Co.), 1-benzylimidazole (Aldrich), and *N*-acetyl-L-histidine (Sigma) were used as received.

Measurements. Proton NMR spectra were recorded at 90 MHz using a pulsed Fourier transform Bruker HX-90E spectrometer. Carbon-13 spectra were recorded on the same instrument at 22.6 MHz. Temperature calibration for proton spectroscopy made use of the Van Geet thermometer.[32] The calibration was verified for carbon-13 measurements by indirect use of the same method.[33] Tetramethylsilane (Me_4Si) was used as an internal reference and downfield shifts from TMS are given positive sign.

Solution magnetic measurements were made by the Evans' method.[34] The proton NMR tube contained a chloroform–1% Me_4Si solution 0.02 M in iron(III) porphyrin and 0.1 to 0.2 M in imidazole ligand. The capillary reference solution was otherwise identical, except a cobalt(III) complex was substituted for the iron(III) complex. Deletion of the cobalt(III) species and use of appropriate constants for diamagnetic correction[35] yielded equivalent magnetic moments. Solvent density changes with temperature were taken into account.[36]

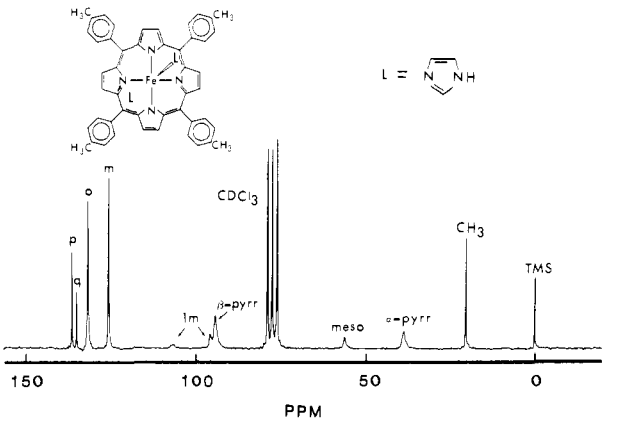

Figure 1. Carbon-13 NMR spectrum of [FeTPP(*p*-CH_3)$(Im)_2$]Cl, 26 °C, $CDCl_3$ solvent.

Results

Addition of imidazoles to solutions of iron(III) porphyrin halide derivatives serves to convert the high-spin species to a low-spin bis(imidazole)-ligated complex.[2,9,37,38] Equilibrium constants are on the order of 10^3 M^{-2} for 1-methylimidazole and 10^6 M^{-2} for imidazole binding to FeTPPCl in chloroform solution at 25 °C.[9,38] Availability of equilibrium constants from previous proton NMR and visible–ultraviolet spectroscopic studies allowed choice of solution conditions for this work such that at least 99% of the iron porphyrin was in the bis-ligated form. Dynamics of imidazole binding previously measured by proton NMR analysis[10] were in part verified (vide infra) in this work. Possible ligand exchange was either avoided (at low temperatures) or accounted for in measurement of bound imidazole resonance values.

A representative carbon-13 NMR spectrum of [FeTPP(*p*-CH_3)$(Im)_2$]Cl is shown in Figure 1. The relatively short electronic relaxation time for low-spin iron(III) allows observation of well-resolved NMR signals for this spin state. However, sizable upfield shifts and line broadening are noted for carbon atoms close to the iron center. Assignments in Figure 1 and in other spectra were made in part by consideration of diamagnetic metalloporphyrin spectra[14-19] and those of bis-cyano complexes.[15-17,20] Other information pertinent to assignments was gained from variable-temperature measurements, line widths, off-resonance broadband and selective frequency decoupling experiments, and examination of variously substituted porphyrins and imidazole derivatives.

Concentration Dependence. Certain porphyrin compounds are known to exhibit aggregation effects at higher concentrations.[19c,39,40] Accordingly, solutions of [FeTPP(*p*-CH_3)$(1\text{-MeIm})_2$]Cl were evaluated for possible concentration dependence at five concentrations ranging from 0.005 to 0.10 M in $CDCl_3$ solvent (Supplementary Tables S1 and S2). The concentration of 1-MeIm was held constant at 0.2 M. Carbon-13 NMR spectra were recorded at both 2 and −45 °C. The chemical shifts were essentially independent of concentration over the temperature range examined. Line widths were essentially constant for concentrations between 0.005 and 0.05 M. However, phenyl line

(23) Adler, A.D.; Longo, F.R.; Finarelli, J.D.; Goldmacher, J.; Assour, J.; Korsakoff, L. *J. Org. Chem.* **1967**, *32*, 476.
(24) Fuhrhop, J.-H.; Smith, K.M. In ref 7, pp 765–769.
(25) Adler, A.D.; Longo, F. R.; Varadi, V., In "Inorganic Synthesis"; Basolo, F., Ed.; McGraw-Hill: New York, 1976; Vol. 16, pp 213–220.
(26) O'Keeffe, D.H.; Barlow, C.H.; Smythe, G.A.; Fuchsman, W.H.; Moss, T.H.; Lilienthal, H.R.; Caughey, W.S. *Bioinorg. Chem.* **1975**, *5*, 125–147.
(27) Scheidt, W.R.; Cunningham, J.A.; Hoard, J.L. *J. Am. Chem. Soc.* **1973**, *95*, 8289–8294.
(28) Lauher, J.W.; Ibers, J.A. *J. Am. Chem. Soc.* **1974**, *96*, 4447–4452.
(29) Gouedard, M.; Gaudemer, F.; Gaudemer, A.; Riche, C. *J. Chem. Res., Synop.* **1978**, 30–31.
(30) Bonnett, R.; Dimsdale, M.J. *J. Chem. Soc., Perkin Trans. 1* **1972**, 2540–2548.
(31) Johnson, A.W.; Kay, I.T. *J. Chem. Soc.* **1960**, 2979–2983.
(32) Van Geet, A.L. *Anal. Chem.* **1968**, *40*, 2227–2229.
(33) Pearson, G.A.; Vietti, D.E. *Anal. Chem.* **1978**, *50*, 1717–1719.
(34) Evans, D.F. *J. Chem. Soc.* **1959**, 2003–2005.
(35) Eaton, S.S.; Eaton, G.R. *Inorg. Chem.* **1980**, *19*, 1095–1096.
(36) "International Critical Tables"; Washburn, E.W., Ed.; McGraw-Hill: New York, 1928; Vol. 3, p 27.
(37) Walker, F.A.; La Mar, G.N. *Ann. N.Y. Acad. Sci.* **1973**, *206*, 328–348.
(38) Walker, F.A.; Lo, M.-W.; Ree, M.T. *J. Am. Chem. Soc.* **1976**, *98*, 5552–5560.
(39) White, W.I. In ref 8, Vol, V, Chapter 7.
(40) Viscio, D.B.; La Mar, G.N. *J. Am. Chem. Soc.* **1978**, *100*, 8092–8096, 8096–8100.

Table I. Dependence of Carbon-13 Resonances on Phenyl Substituents[a]

phenyl subst	carbon atom α-pyrrole[b]	β-pyrrole[c]	meso[b]
H	13.7	86.6	37.5
m-CH_3	14.1	86.7	38.0
p-CH_3	14.9	87.5	39.1
p-OCH_3	14.8	87.5	39.2
o-CH_3	15.3	88.0	38.0

[a] [FeTPP(R)(1-MeIm)$_2$]Cl, 0.05 M; −22 °C; TMS ref; $CDCl_3$ solvent. [b] Uncertainties ca. ±0.3 ppm. [c] Uncertainties ca. ±0.2 ppm.

widths are approximately doubled at 0.10 M. Other porphyrin and imidazole resonances are broadened to a lesser, but significant extent at this high concentration. Absence of chemical shift changes suggests that line broadening results from increases in solution viscosity and bulk susceptibility rather than specific porphyrin aggregation. Phenyl resonances show proportionally larger broadening due to initially smaller line widths.

Ligand Exchange Kinetics. The ligand exchange rate for 5-methylimidazole binding to [FeTPP(p-CH_3)(5-MeIm)$_2$]Cl was determined from line broadening in the slow exchange region. The quaternary carbon line width of 5-MeIm was measured at varying temperatures for chloroform solutions 0.05 M in iron porphyrin and 0.20 M in total ligand. A complete tabulation of spectra is found in Supplementary Table S3. Line widths in hertz are listed in parentheses at the following temperatures: −45 °C (17 Hz), −22 °C (12), 2 °C (7), 26 °C (9), 35 °C (14), 39 °C (18). Extrapolation of the low-temperature values yields the bound ligand line width, $\Delta\nu_{1/2}$, in the exchange region. The preexchange lifetime, τ, is then given by [10]

$$\tau = \frac{1}{\pi(\Delta\nu_{1/2}(\text{obsd}) - \Delta\nu_{1/2})} \quad (1)$$

where $\Delta\nu_{1/2}$(obsd) is the observed line width at exchange. From the line widths listed above, an apparent exchange rate constant, τ^{-1}, of 12 ± 3 s^{-1} at 25 °C is estimated. This value is equivalent to the value of 14 ± 2 s^{-1} previously obtained for [FeTPP(5-MeIm)$_2$]Cl by proton NMR analysis under slightly different solution conditions.[10]

Dependence on Phenyl Substituents. The electron-releasing/withdrawing nature of phenyl substituents in the FeTPP(R) series is known to affect physiochemical properties such as ligand binding constants[9,38] and redox potentials.[41,42] A small but significant effect is also apparent in the carbon-13 resonance positions listed in Table I (complete spectral listings at both −22 and 26 °C are included as supplementary material (tables S4–S8). Thus, in terms of the σ constant, which provides a measure of inductive and resonance effects, the substituent order for Table I should be H > m-CH_3 > p-CH_3 > p-OCH_3 ~ o-CH_3. This general trend is indeed apparent in that the upfield shifts of pyrrole, and meso resonances are smaller for the more strongly electron-releasing substituents. Corresponding resonances for diamagnetic cobalt(III) complexes (vide infra) are not measurably sensitive to phenyl substituents.

Imidazole complexes of FeTPP(R)Cl derivatives were also examined by proton NMR spectroscopy under the same solution conditions (0.05 M in iron porphyrin) employed for carbon-13 measurements. Results (tabulated in Supplementary Table S9) were equivalent to those previously obtained by La Mar and co-workers.[2,3,9-11] Such spectra were recorded to allow direct comparison of proton and carbon-13 isotropic shift values in the analysis of isotropic shifts discussed later.

Dependence on Imidazole Substitution. Effects of variously substituted imidazoles on the magnitude of porphyrin resonance values are summarized in Table II. Complete lists of resonances are included in Supplementary Tables S3, S6, and S10–S12. The β-pyrrole carbon signal shows the greatest sensitivity to imidazole substitution with shift differences up to 6.6 ppm for 1-methyl- vs. 5-methylimidazole. Use of a 2:1 chloroform–methanol mixture (required for dissolution of N-acetyl histidine) had no significant effect on resonance positions for the imidazole complex as demonstrated by the first and last entries in Table II.

Table II. Dependence of Carbon-13 Resonances on Imidazole Substitution[a]

ligand	carbon atom α-pyrrole[b]	β-pyrrole[c]	meso[b]
Im	15.5	85.1	38.7
1-MeIm	14.9	87.5	39.1
5-MeIm	14.0	81.0	38.0
1-BzIm	14.0	87.3	40.0
N-AcHis[d]	15.0	84.0	39.0
Im[d]	14.9	85.4	38.5

[a] [FeTPP(p-CH_3)(R-Im)$_2$]Cl, 0.05 M; −22 °C; TMS ref; $CDCl_3$ solvent. [b] Uncertainties ca. ±0.3 ppm. [c] Uncertainties ca. ±0.2 ppm. [d] 2:1 $CDCl_3$–CH_3OH solvent.

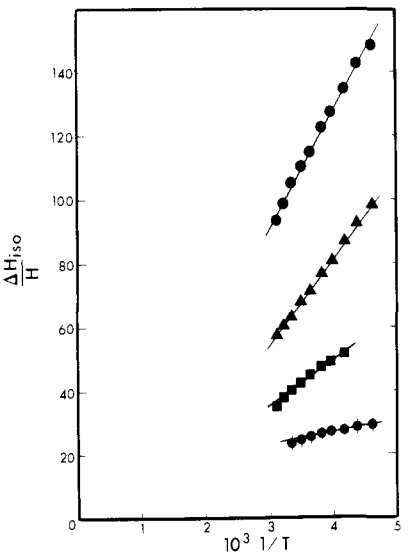

Figure 2. Curie law plot of carbon-13 resonances in [FeTPP(p-CH_3)-(Im)$_2$]Cl: (●) α-pyrrole carbon; (▲) meso carbon; (■) β-pyrrole carbon; (◆) imidazole-5-carbon. Lines are illustrative only.

Effects of changing the iron(III) porphyrin counterion were investigated in a cursory manner by using FeTPPBr to generate the [FeTPP(1-MeIm)$_2$]Br complex. At 2 °C pyrrole and meso-carbon signals were not measurably different from those of the chloride analogue. However, small differences were detected for the phenyl signals, in which case the bromide complex resonances were an average of 0.3 ppm further downfield. This subtle effect is thought to reflect differences in chloride and bromide ion pair structure or energetics.

Variable-Temperature Studies. Carbon-13 NMR spectra of [FeTPP(p-CH_3)(Im)$_2$]Cl in $CDCl_3$ solution were recorded over the accessible temperature range of the solvent. Resonance values are tabulated in Supplementary Table S12. Isotropic shift values are readily obtained by subtracting the chemical shift of the respective carbon atom in an analogous diamagnetic cobalt(III) complex. Curie plots of such isotropic shift values are presented in Figures 2 and 3. Curvature and nonzero intercepts were also apparent in Curie plots for the [FeTPP(1-MeIm)$_2$]Cl complex.

Cobalt(III) Porphyrins. Cobalt(III) porphyrin–imidazole complexes were employed as diamagnetic reference compounds. Eaton and Eaton have pointed out the need for judicious choice of carbon-13 diamagnetic references when isotropic shifts are small.[18] Accordingly, the cobalt(III) complexes seem more appropriate references for six-coordinate iron porphyrins than the square-planar nickel(II) porphyrins[2] or ruthenium(II) porphy-

(41) Walker, F.A.; Beroiz, D.; Kadish, K.M. *J. Am. Chem. Soc.* **1976**, *98*, 3484–3489.
(42) Kadish, K.M.; Bottomley, L.A.; Beroiz, D. *Inorg. Chem.* **1978**, *17*, 1124–1129.

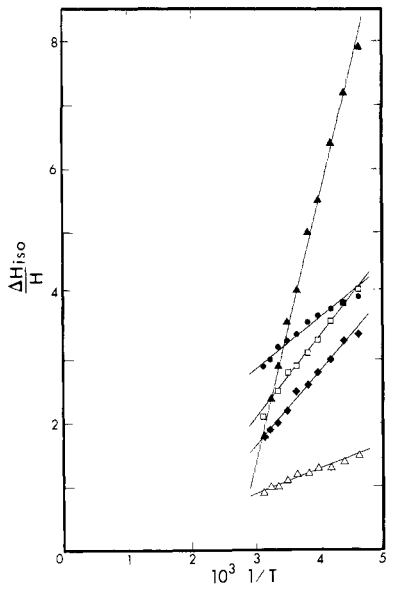

Figure 3. Curie law plot of carbon-13 resonances in [FeTPP(p-CH_3)-$(Im)_2$]Cl: (▲) ortho carbon; (●) quaternary carbon at meso; (□) meta carbon; (■) para carbon; (△) phenyl-CH_3. Lines are illustrative only.

Table III. Carbon-13 NMR Spectra of [CoTPP(R)(1-MeIm)$_2$] Cl Complexes[a]

carbon atom	CoTPP	CoTPP(m-CH_3)	CoTPP(p-CH_3)
phenyl at meso	140.5	140.5	137.6
ortho	134.1	135.0, 131.5	134.0
meta	127.1	136.6, 126.8	127.7
para	128.2	128.9	137.9
phenyl-CH_3		21.6	21.4
meso	119.9	119.9	119.8
α-pyrrole	143.1	143.1	143.1
β-pyrrole	134.6	134.5	134.4
Im-2-C	132.1	132.0	132.1
Im-4-C	123.2	123.1	123.2
Im-5-C	119.0	119.0	118.8
Im-CH_3	33.8	33.7	33.7

[a] Complex, 0.05 M; 26 °C; TMS ref; $CDCl_3$ solvent; uncertainties ±0.1 ppm.

rin–imidazole complexes[3] previously used for proton spectroscopy. The possibility of small second-order Zeeman contributions to cobalt(III) chemical shifts cannot be ruled out. However, the overall results presented here would be affected to only a minor degree if a ZnTPP diamagnetic reference were employed, as the maximum difference in phenyl carbon resonance values is 0.8 ppm.[16]

Cobalt(III) porphyrin–imidazole complexes were prepared and isolated in the solid state. A large equilibrium constant for imidazole binding and slow imidazole exchange on the NMR time scale permitted dissolution in $CDCl_3$ and direct observation of carbon-13 NMR resonances. Assignments were made based on literature reports of other diamagnetic porphyrins, combined with examination of phenyl-substituted derivatives, and consideration of expected upfield ring current shifts of coordinated imidazoles. Carbon-13 resonances have been previously reported for coordinated 1-methylimidazole.[43] A representative spectrum is shown in Figure 4. Carbon-13 resonance values listed in Table III are used for the isotropic shift analysis in this report, and should provide diamagnetic references for other paramagnetic metalloporphyrin studies. Chemical shift values were temperature independent (within ±0.2 ppm) over the range from −22 to 26 °C. Proton NMR spectra of cobalt(III) complexes were likewise recorded (Supplementary Table S13) to provide suitable diamagnetic reference values.

(43) Gouedard, M.; Gaudemer, F.; Gaudemer, A. *Tetrahedron Lett.* **1973**, 2257–2260.

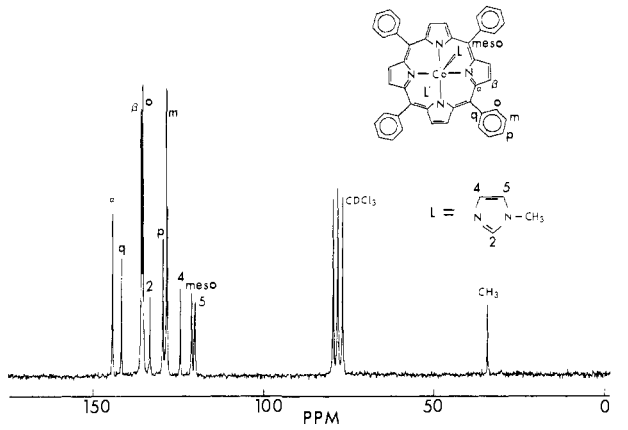

Figure 4. Carbon-13 NMR spectrum of [CoTPP(1-MeIm)$_2$]Cl, 26 °C, $CDCl_3$ solvent.

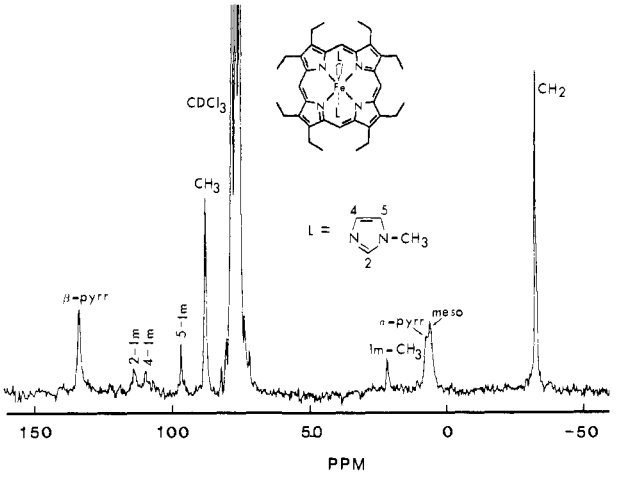

Figure 5. Carbon-13 NMR spectrum of [FeOEP(1-MeIm)$_2$]Cl, −22 °C, $CDCl_3$ solvent.

Table IV. Carbon-13 NMR of FeOEPCl Complexes[a]

	1-MeIm complex			5-MeIm complex		
carbon atom	26 °C[b]	2 °C[b]	−22 °C[c]	26 °C[b]	2 °C[c]	−22 °C[c]
α-pyrrole	45.4	24.8	7.3	37.1	21.7	6.5
β-pyrrole	146.7	138.7	133.7	131.9	127.2	124.3
meso	23.6	16.7	6.2	25.0	18.0	8.4
CH_2	−23.6	−27.2	−32.4	−20.9	−24.8	−29.6
CH_3	*d*	82.8	88.2	72.9	*d*	83.3
Im-2-C	*e*	120.1	114.1	*e*	98.0	93.0
Im-4-C	*e*	112.8	109.4	*e*		
Im-5-C	*e*	101.8	96.9	*e*	111.0	107.2
Im-CH_3	*e*	24.1	22.0	*e*	0.4	−0.5

[a] FeOEPCl, 0.04 M; TMS ref; $CDCl_3$ solvent. [b] Ligand 0.16 M. [c] Ligand 0.08 M. [d] Signal is under solvent. [e] Chemical shifts could not be accurately measured owing to an intermediate-rate ligand exchange process.

Pyrrole-Substituted Synthetic Metalloporphyrins. Pyrrole-substituted synthetic porphyrins resemble natural porphyrins more closely and were examined in part to facilitate assignments and verify shift patterns for the latter compounds. Derivatives of octaethylporphyrin and etioporphyrin I were utilized. A representative carbon-13 spectrum of [FeOEP(1-MeIm)$_2$]Cl at −22 °C is shown in Figure 5 and additional spectral data are included in Table IV. Assignments were made in part by a gated decoupling experiment which revealed the following carbon–proton splittings (ppm): −32.4, triplet; 6.2, doublet; 22.0, quartet; 88.2, quartet; and 96.9, doublet. Quaternary carbon resonances at 7.3 and 133.7 ppm are assigned to α- and β-pyrrole carbon atoms on the basis of line width, and in the case of the 7.3-ppm peak, by analogy with FeTPP spectra. Axial ligand resonances are also

Table V. NMR of Etioporphyrin I Derivatives[a]

group	[CoETIO-(1-MeIm)$_2$]Cl carbon[b]	[CoETIO-(1-MeIm)$_2$]Cl proton[b]	[FeETIO-(1-MeIm)$_2$]Cl carbon[c]	[FeETIO-(1-MeIm)$_2$]Cl proton[d]
α-pyrrole	146.2		43.0	
β-pyrrole	141.8		147.5	
meso	96.7	10.25	23.5	3.10
ring CH_3	12.2	3.70	−34.6	15.99
ring CH_2	20.3	4.14	−23.2	6.80
CH_2CH_3	17.9	1.87	*e*	−0.23
Im-2-CH	132.0	−0.02	*f*	*f*
Im-4-CH	122.8	−0.45	*f*	*f*
Im-5-CH	118.1	4.36	*f*	*f*
Im-CH_3	33.3	1.87	*f*	*f*

[a] 26 °C, TMS ref, $CDCl_3$ solvent. [b] Ca. 5 mM. [c] FeETIOCl ca. 0.02 M, 1-MeIm 0.20 M. [d] FeETIOCl ca. 0.02 M, 1-MeIm 0.05 M. [e] Signal is under solvent. [f] Chemical shifts could not be accurately measured owing to an intermediate-rate ligand exchange process.

assigned by comparison of FeTPP shift patterns, although differences of up to 7 ppm are noted for axial ligand resonances of the two porphyrin structural types (cf. Tables S4 and S5 with Table IV). The nature of the axial ligand also affects the OEP resonance values, as demonstrated in Table IV for 1-MeIm and 5-MeIm ligands. The β-pyrrole carbon resonance is especially sensitive, with differences of up to 15 ppm for the two complexes. Curie plots of the limited variable-temperature data reported in Table IV reveal sizable deviations for pyrrole resonances and more nearly ideal behavior for meso and ethyl signals. Note that the methyl resonance of OEP is shifted downfield unlike other porphyrin and axial ligand signals which experience an upfield isotropic shift.

Etioporphyrin I has a fourfold symmetric structure with alternating ring methyl and ethyl groups. Although ETIO complexes have not been utilized to a large extent in NMR studies, the presence of the ring methyl group makes this compound a more appropriate analogue of the natural porphyrins than OEP derivatives. The lower solubility of ETIO complexes does, however, dictate longer spectral acquisition times, and precluded low-temperature carbon-13 measurements. Carbon-13 and proton NMR results are included in Table V. Carbon-13 assignments for the cobalt(III) diamagnetic reference compound were made by comparison of TIOEP spectra and axial ligand resonances of CoTPP complexes. Assignments for the iron(III) complex follow from those for FeOEP.

Natural-Derivative Iron Porphyrins. Carbon-13 NMR spectra have previously been reported for iron(III) cyanide (or perhaps cyanide/pyridine[17]) complexes of protoporphyrin, deuteroporphyrin,[17,20] 2,4-dibromodeuteroporphyrin,[20] 2,4-diacetyldeuteroporphyrin,[20] and hemin *c*.[15] Corresponding spectra for 1-methylimidazole complexes exhibit similar shift patterns. A representative spectrum of iron protoporphyrin is shown in Figure 6, and selected resonance values for various natural-porphyrin

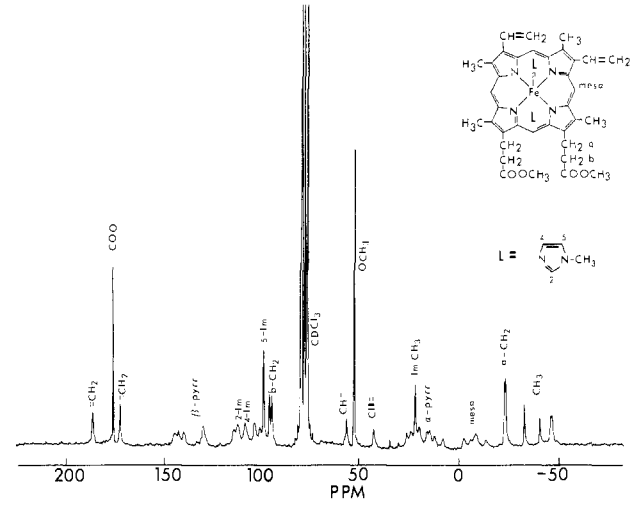

Figure 6. Carbon-13 NMR spectrum of [FeProtDME(1-MeIm)$_2$]Cl, −22 °C, $CDCl_3$ solvent.

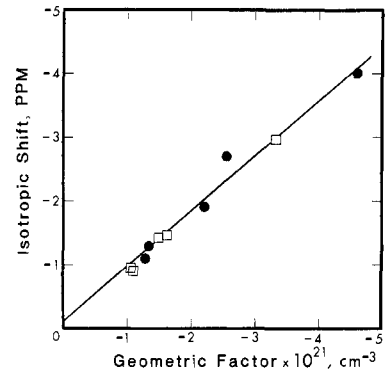

Figure 7. Plot of isotropic shifts vs. geometric factors for 1-MeIm complexes of FeTPP(R)Cl, 26 °C, $CDCl_3$ solvent: (●) carbon-13 values, (□) proton values.

derivatives are listed in Table VI. At −22 °C coordinated ligand resonances are observed in the slow exchange limit, and the iron porphyrin is completely ligated (>99%). Assignments were verified by comparison with FeOEP and FeETIO complexes, through substitution of 2,4-R groups, by variable-temperature measurements, and by selective frequency decoupling experiments.

Discussion

For a paramagnetic substance the isotropic NMR shift is defined as the difference in ppm for a resonance in the paramagnetic complex vs. the value for a suitable diamagnetic reference compound. Carbon-13 isotropic shifts are composed of three parts[44]

$$\frac{\Delta H_{iso}}{H} = \frac{\Delta H_{con}}{H} + \frac{\Delta H_{dip}^{LC}}{H} + \frac{\Delta H_{dip}^{MC}}{H} \quad (2)$$

Table VI. Selected Carbon-13 NMR Resonances for Iron(III) Natural Porphyrin-1-Methylimidazole Complexes[a]

carbon atom	FeMesoDME	FeProtDME	FeDeutDME	FeAcDME
ring CH_3	−38.4, −45.1, −45.1, −51.7	−34.1, −42.5, −48.8, −49.1	−32.3, −39.8, −47.4, −51.1	−17.7, −23.9, −50.7, −59.6
mean value	−45.1	−43.6	−42.7	−38.0
av dev from mean	3.3	5.3	6.6	17.2
prop CH_2				
(a)	−24.2, −24.8	−24.0, −24.5	−21.2, −26.6	−17.0, −25.2
(b)	96.0, 94.5	94.9, 93.7	98.5, 88.4	96.0
COO	174.8	174.7	174.8, 174.3	174.5, 174.3
OCH_3	51.8	51.9	51.9	51.9
2,4-R	−26.6, −38.4[b]	55.7, 37.8[d]		159.1, 155.0[f]
	c	184.5, 171.3[e]		27.4[g]
Im-CH_3	21.7	21.0	20.8	19.0
Im-5-C	97.6	97.9	96.6	99.3

[a] Iron(III) prophyrin, 0.05 M; 1-MeIm, 0.2 M; −22 °C; TMS ref, $CDCl_3$ solvent. [b] Ring CH_2. [c] CH_3 signal is under solvent. [d] CH=. [e] CH_2=. [f] C=O. [g] CH_3.

Table VII. Separation of Contact and Dipolar Shift Terms[a]

carbon atom	carbon-13 $\frac{3\cos^2\theta-1}{r^3}\times 10^{21}$	carbon-13 $\frac{\Delta H_{iso}}{H}$	carbon-13 $\frac{\Delta H_{dip}^{MC}}{H}$	carbon-13 $\frac{\Delta H_{con}}{H}+\frac{\Delta H_{dip}^{LC}}{H}$	proton $\frac{\Delta H_{con}}{H}$
ortho	−4.61	−4.0	−4.1	~0	~0
meta	−2.55	−2.7	−2.3	~0	~0
para	−2.20	−1.9	−2.0	~0	~0
m-CH_3	−1.32	−1.3	−1.3	~0	~0
p-CH_3	−1.28	−1.1	−1.2	~0	~0
phenyl-C at meso	−8.4	−3.2	−7.3	+4	
meso (TPP)	−25	−65	−22	−43	
meso (ETIO)	−25	−73.2	−22	−51.2	+2.43 (+2.3[b])
α-pyrrole (TPP)	−36	−101.5	−31	−70	
β-pyrrole (TPP)	−13.0	−36.0	−11	−25	−19.67 (−19.5[b])
pyrrole-CH_3	−5.6	−46.8	−5.0	−42	+16.08
pyrrole-CH_2	−5.6	−43.5	−5.0	−39	+6.45 (+5.2[b])
pyrrole-CH_2CH_3	−3.0	+60	−2.7	+63	
1m-2-C	+62	−13[c]	+53	−66	(−28.0[d])
Im-4-C	+59	−12[c]	+51	−63	(−8.2[d])
1m-5-C	+27	−16.7[c]	+23	−40	(−7.6[d])
1m-1-CH_3	+12	−11.0[c]	+10	−21	(+10.3[d])
1m-5-CH_3[e]	+10	−9.7[c]	+9	−19	(+9.0[d])

[a] 1-MeIm complexes of iron(III) porphyrins, 26 °C, $CDCl_3$ solvent. [b] Reference 2, 29 °C. [c] FeTPP complexes; extrapolated from low temperatures where ligand exchange is slow. [d] Reference 3, 25 °C. [e] 5-MeIm complex.

where $\Delta H_{con}/H$ is the contact contribution, $\Delta H_{dip}^{LC}/H$ is a ligand-centered dipolar shift, and $\Delta H_{dip}^{MC}/H$ is a metal-centered dipolar shift. For protons the $\Delta H_{dip}^{LC}/H$ term is expected to be negligible. For the limiting case of axial symmetry, the metal-centered dipolar shift is defined by (with downfield shifts given a positive sign)[45]

$$\frac{\Delta H_{dip}^{MC}}{H} = \frac{1}{3N}(\chi_\parallel - \chi_\perp)\frac{3\cos^2\theta - 1}{r^3} \qquad (3)$$

where N is Avogadro's number and χ values refer to molecular susceptibilities. The $(3\cos^2\theta - 1)/r^3$ term (geometric factor) defines the position of the observed nucleus with respect to the molecular axis and metal center. Separation of contact and dipolar contributions for proton isotropic shifts in low-spin iron(III)[2] and intermediate-spin iron(II)[46] has relied on the assumption that phenyl protons experience only dipolar shifts. A test of this hypothesis is found in the correspondence of phenyl proton isotropic shifts and calculated geometric factors.[2,46,47] As expected, a resonable correspondence is also observed (see Figure 7) for phenyl and tolyl carbon-13 isotropic shifts, with carbon and proton values being essentially colinear. In each case the [CoTPP(R)(1-MeIm)$_2$]Cl complexes have been used as diamagnetic reference compounds. The curve in Figure 7 represents a best fit for the five carbon resonances. It should be noted that the isotropic shift for the phenyl carbon attached at the meso position (not shown in Figure 7) does not parallel the geometric factor, suggesting a contact contribution at this site.

The value of $\chi_\parallel - \chi_\perp$ taken from the least-squares slope of carbon-13 data in Figure 7 is 1550×10^{-6} cgs unit. Using a solution magnetic moment of 2.30 BM for [FeTPP(Im)$_2$]Cl obtained in this study, a 26 °C $\bar{\chi}$ value of 2194×10^{-6} cgs unit is calculated. Thus, two relationships

$$\chi_\parallel - \chi_\perp = 1550 \times 10^{-6} \text{ cgs unit} \qquad (4)$$

$$\bar{\chi} = \tfrac{1}{3}(\chi_\parallel + 2\chi_\perp) = 2194 \times 10^{-6} \text{ cgs unit} \qquad (5)$$

yield $\chi_\parallel = 3227 \times 10^{-6}$ cgs unit ($\mu_\parallel$ = 2.79 BM) and $\chi_\perp = 1677 \times 10^{-6}$ cgs unit ($\mu_\perp$ = 2.01 BM). The equivalence of carbon-13 and proton results suggested by Figure 7 is further verified by treatment of earlier data,[2] to obtain χ values essentially identical with those calculated above. Although a direct correspondence between susceptibility anisotropy and *g*-tensor anisotropy is not expected for a system showing second-order Zeeman effects or excited state contributions, Horrocks and Greenberg have shown the second-order Zeeman term to be minimal for bis(imidazole) ferrihemoproteins.[22] Calculation of ESR *g* values from

$$g_i = \mu_i[S(S+1)]^{-1/2} \qquad (6)$$

yields $g_\parallel$ = 3.2 and $g_\perp$ = 2.3. Frozen-glass ESR spectra are rhombic, with g_1 = 2.92, g_2 = 2.30, and g_3 = 1.56.[11] Combination of g_2 and g_3 values yields $g_\parallel$ = 2.92 and $g_\perp$ = 1.93. Calculation of $g_\parallel^2 - g_\perp^2$ values of 5.0 (NMR) and 4.8 (ESR) gives perhaps a better comparison of the total anisotropy measured by the two physical methods, as noted previously.[2]

Having shown that carbon-13 and proton phenyl shifts are represented by the metal-centered dipolar term, it is possible to estimate this contribution for any atom in the porphyrin molecule simply by consideration of appropriate geometric factors and eq 3. Structural information for [FeTPP(Im)$_2$]Cl is available.[48] Table VII lists calculated geometric factors and metal-centered dipolar shift values for various porphyrin and axial ligand carbon-13 resonances. Differences between observed isotropic shifts and metal-centered dipolar shifts are the sum of the contact shift and ligand-centered dipolar shift. This sum is compared with the correspondingly determined contact shift for protons listed in the last column of Table VII.

Qualitative relationships exist between the observed contact shifts for carbon atoms and attached protons.[44] In particular, if unpaired spin density is located in a σ-type MO, both carbon and proton shifts are expected to be downfield. (However, for nuclei close the the metal center, an indirect or spin polarization mechanism may cause alternation in the direction of shifts.) For spin density in a π-type MO, carbon and attached proton contact shifts should be of opposite sign. Unpaired spin delocalization through a π-type MO is expected to be predominant for low-spin iron(III) complexes.[2] This dictates that, for example, the β-pyrrole carbon and attached proton contact shifts should be opposite in sign. The fact that β-pyrrole carbon $\Delta H_{con}/H + \Delta H_{dip}^{LC}/H$ and attached proton $\Delta H_{con}/H$ values are of the same sign suggests that the carbon $\Delta H_{dip}^{LC}/H$ term is comparable in magnitude to the

(44) McGarvey, B.R.; Kurland, R.J. In "NMR of Paramagnetic Molecules"; La Mar, G.N.; Horrocks, W.DeW.; Holm, R.H., Eds.; Academic Press: New York, 1973; Chapter 14.
(45) Horrocks, W.DeW. In ref 44, Chapter 4.
(46) Goff, H.; La Mar, G.N.; Reed, C.A. *J. Am. Chem. Soc.* **1977**, *99*, 3641–3646.
(47) Goff, H.; La Mar, G.N. *J. Am. Chem. Soc.* **1977**, *99*, 6599–6606.
(48) Collins, D.M.; Countryman, R.; Hoard, J.L. *J. Am. Chem. Soc.* **1972**, *94*, 2066–2072.

carbon contact term. Consideration of both carbon and proton isotropic shift data for the general relationships derived by Karplus and Fraenkel[21] allows estimation of these individual shift contributions. This approach has previously been attempted by Wüthrich and Baumann[16] for iron porphyrins, but uncertainties resulted from the inability to separate the metal-centered dipolar term.

The proton hyperfine coupling constant, A^H, is proportional to the unpaired spin density, ρ^π_C, centered on the π orbital of the carbon atom to which it is attached. Quantitatively these two values are related by the total spin, S, and a constant[44]

$$A^H = \frac{Q^H_{CH}\rho^\pi_C}{2S} \tag{7}$$

where the empirical value of Q^H_{CH} is approximately -63 MHz. For a case in which the Curie law is valid, the value of A^H is defined by the contact shift according to

$$\frac{\Delta H_{con}}{H} = A^H\frac{|\gamma_e|}{|\gamma_H|}\frac{S(S+1)}{3kT} \tag{8}$$

where γ_e and γ_H are the gyromagnetic ratios of the electron and proton, respectively. Using eq 7 and 8 along with pyrrole proton and meso-proton contact shifts of -19.67 and +2.43 ppm, carbon π-spin density values of 0.012 (β carbon) and -0.0015 (meso carbon) are obtained. Carbon contact shifts result from unpairing of carbon 1s electrons and unpairing of the three carbon sp^2 bonding pairs. Contact shifts for β-pyrrole and meso-carbon atoms may be defined by the Karplus and Fraenkel relationships[21,49]

$$\frac{\Delta H_{con(\beta)}}{H} = [(S^C + 2Q^C_{CC'} + Q^C_{CH})\rho^\pi_\beta + Q^C_{C'C}(\rho^\pi_\beta + \rho^\pi_\alpha)]\frac{|\gamma_e|}{|\gamma_C|}\frac{S(S+1)}{3kT} \tag{9}$$

$$\frac{\Delta H_{con(meso)}}{H} = [(S^C + 2Q^C_{CC'} + Q^C_{CH})\rho^\pi_{meso} + 2Q^C_{C'C}\rho^\pi_\alpha]\frac{|\gamma_e|}{|\gamma_C|}\frac{S(S+1)}{3kT} \tag{10}$$

The S^C term reflects polarization of the 1s orbital. Polarization of the three sp^2 bonds by π-spin density centered on the observed carbon atom is accounted for by the $Q^C_{CC'}$ and Q^C_{CH} terms. The $Q^C_{C'C}$ term represents polarization of the two carbon–carbon bonds by spin density centered on neighboring carbon atoms. Reasonable values obtained from π-radical systems are: S^C, -35.5 MHz; $Q^C_{CC'}$, +40.3 MHz; Q^C_{CH}, +54.6 MHz; and $Q^C_{C'C}$, -39 MHz.[21] Slightly different constants (or sums of constants) have recently been proposed. Strom et al., have calibrated values largely on Q^C_{CH} for the methyl radical.[50] Neely et al. evaluated combined proton and carbon-13 NMR data for imino nitroxide radicals, but did not take into consideration ligand-centered carbon-13 dipolar shifts.[51] Thus, the more recently determined constants appear to be no more representative than those originally tabulated by Karplus and Fraenkel. The original values listed above were utilized in this study.[21]

Note that direct calculation of contact shift values by eq 9 and 10 requires knowledge of the ρ^π_α value. Indirect solution is, however, possible by including values of $\Delta H_{con}/H + \Delta H^{LC}_{dip}/H$ from Table VII. The ligand-centered dipolar term is assumed

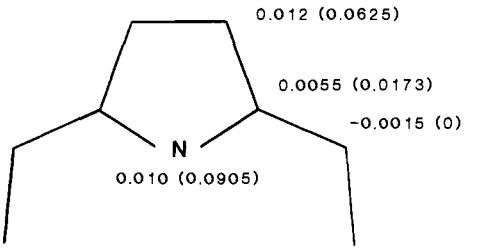

Figure 8. Calculated spin densities at porphyrin carbon and nitrogen atoms. Values in parentheses are average Hückel electron densities (one electron per porphyrin).

to be direclty related to the spin density at the observed carbon by a constant, D, such that

$$\frac{\Delta H^{LC}_{dip(\beta)}}{H} = D\rho^\pi_\beta \tag{11}$$

$$\frac{\Delta H^{LC}_{dip(meso)}}{H} = D\rho^\pi_{meso} \tag{12}$$

Combination of these equations with eq 9 and 10 yields

$$\frac{\Delta H_{con(\beta)}}{H} + \frac{\Delta H^{LC}_{dip((\beta)}}{H} = D\rho^\pi_\beta + [(S^C + 2Q^C_{CC'} + Q^C_{CH})\rho^\pi_\beta + Q^C_{C'C}(\rho^\pi_\beta + \rho^\pi_\alpha)]\frac{|\gamma_e|}{|\gamma_C|}\frac{S(S+1)}{3kT} \tag{13}$$

$$\frac{\Delta H_{con(meso)}}{H} + \frac{\Delta H^{LC}_{dip(meso)}}{H} = D\rho^\pi_{meso} + [(S^C + 2Q^C_{CC'} + Q^C_{CH})\rho^\pi_{meso} + 2Q^C_{C'C}\rho^\pi_\alpha]\frac{|\gamma_e|}{|\gamma_C|}\frac{S(S+1)}{3kT} \tag{14}$$

Simultaneous solution of these relationships provides a D value of -6567 ppm per one unpaired spin, and a ρ^π_α value of +0.0055. (The constancy of D is being evaluated for spin states in other metalloporphyrins.) The pyrrole nitrogen spin density, $\rho^\pi_N = 0.010$ is estimated from a similar relationship

$$\frac{\Delta H_{con(\alpha)}}{H} + \frac{\Delta H^{LC}_{dip(\alpha)}}{H} = D\rho^\pi_\alpha + [(S^C + 2Q^C_{CC'} + Q^C_{CN})\rho^\pi_\alpha + Q^C_{C'C}(\rho^\pi_\beta + \rho^\pi_{meso}) + Q^C_{NC}\rho^\pi_N]\frac{|\gamma_e|}{|\gamma_C|}\frac{S(S+1)}{3kT} \tag{15}$$

where the assumptions $Q^C_{CN} = Q^C_{CC'}$ and $Q^C_{NC} = Q^C_{C'C}$ are made.[51]

Spin density values for the porphyrin skeleton are summarized in Figure 8. Spin density at the β-pyrrole carbon is identical with that previously determined by Shulman et al. for iron(III) porphyrin–cyanide complexes.[52] The meso-carbon spin density of -0.0015 is approximately one-half that calculated in the earlier work. Along with the experimental spin densities in Figure 8 are listed in parentheses the expected average Hückel electron densities (one unpaired spin per porphyrin) for the $3e(\pi)$ molecular orbitals.[53] This is a filled MO and unpaired spin delocalization is presumably via porphyrin → iron charge transfer. Agreement with calculation is qualitative in the sense that spin density is concentrated at the pyrrole nitrogen and β-pyrrole carbon atoms. Appearance of spin density at the meso-carbon position may be due to mixing of the $4e(\pi)$ MO.[52] Electron correlation effects also provide a realistic explanation for appearance of small negative spin density at the meso position. An upgraded calculation which includes electron correlation would be of some value in evaluating the NMR shift analysis.

(49) Note in ref 16 that the last part of the relationship was incorrectly deleted, but the complete equation was apparently utilized in the calculations.

(50) Strom, E.T; Underwood, G.R.; Jurkowitz, D. *Mol. Phys.* **1972**, *24*, 901–904.

(51) Neely, J.W.; Lam, C.H; Kreilick, R.W. *Mol. Phys.* **1975**, *29*, 1663–1671.

(52) Shulman, R.G.; Glarum, S.H.; Karplus, M. *J. Mol. Biol.* **1971**, *57*, 93–115.

(53) Longuet-Higgins, H.C.; Rector, C.W.; Platt, J.R. *J. Chem. Phys.* **1950**, *18*, 1174–1181.

Table VIII. Summary of Contributions to Isotropic and Contact Shifts for Selected Carbon Atoms[a]

	β-pyrr-C[b]	α-pyrr-C	meso-C	pyrr-CH_3
$\Delta H_{iso}/H$	−36.0	−101.5	−73.2	−46.8
$\Delta H^{MC}_{dip}/H$	−11	−31	−22	−5.0
$\Delta H^{LC}_{dip}/H$	−78	−36	+10	
$\Delta H_{con}/H$	+53	−34	−61	−47
	Contributions to Contact Term			
S^C	−44	−21	+5	
$2Q^C_{CC'}$	+100	+47	−12	
Q^C_{CH}	+68		−8	
Q^C_{CN}		+23		
$Q^C_{C'C}\rho^\pi_\beta$	−48	−48		−42
$Q^C_{C'C}\rho^\pi_\alpha$	−23		−45	
$Q^C_{C'C}\rho^\pi_{meso}$		+6		
$Q^C_{NC}\rho^\pi_N$		−41		

[a] 1-MeIm complexes of iron(III) porphyrins, 26 °C. [b] pyrr = pyrrole.

It is instructive to dissect the observed isotropic shifts into individual contributions. Such values are reported in Table VIII. As was noted by Wüthrich and Baumann,[16] the ligand-centered dipolar term is very significant and contributes to an upfield shift for the β-pyrrole carbon atom of FeTPP. The downfield contact shift at this position is, however, consistent with the upfield pyrrole proton contact shift. An unusual situation is apparent for the α-pyrrole carbon atom, in that although the contact shift term is upfield, positive spin density is found at the position. Polarization by neighboring β-pyrrole carbon and pyrrole nitrogen spin serves to account for the upfield shift. The meso-carbon resonance exhibits the smallest spin density (Figure 8), but the largest absolute contact shift. The significant contact shift is once again the consequence of polarization by neighboring α-pyrrole carbon spin density.

Internal consistency of the Karplus and Fraenkel analysis is demonstrated in part through prediction of the ring methyl carbon contact shift value. This carbon atom is not a part of the π system and to first order should have a contact shift term reflecting only polarization of its 2s electrons by π-spin density at the β-pyrrole carbon atom. Thus, the following relation[44]

$$\frac{\Delta H_{con(CH_3)}}{H} = Q^C_{C'C}\rho^\pi_\beta \frac{|\gamma_e|}{|\gamma_C|} \frac{S(S+1)}{3kT} \qquad (16)$$

is employed to calculate a ring methyl contact shift of −48 ppm. The calculated value is in reasonable agreement with the −42 ppm contact shift (Table VII) observed for the ring methyl carbon of FeETIO. Some differences in these two values might be anticipated, as the ρ^π_β term should be measurably different for FeTPP and FeETIO complexes. Alternately it could be argued that the recently determined $Q^C_{C'C}$ values, which are smaller than −39 MHz, give an even better match with the experimental value and in fact should be used.[50,51] The large downfield shifts apparent for β-CH_3 and -CH_2 groups are rationalized by a hyperconjugation mechanism.[17,54]

Adequate data are available to carry out a corresponding analysis of axial imidazole isotropic shifts. However, such an analysis would be persumptive at this time considering the rather poor understanding imidazole π-molecular orbitals.[3]

Analysis of isotropic shift contributions should be considered as a semiquantitative rather than an absolute treatment. Use of available theory originally developed for ESR spectroscopy of organic radicals potentially has shortcomings when applied to NMR spectra of paramagnetic metal complexes. Some uncertainty exists in choice of S^C and Q_i constants, although deviations on the order of 10% would not change the general conclusions drawn from Table VIII. Unpaired spin delocalization through a σ-bond framework and ligand-centered dipolar shifts from neighboring atoms have been assumed negligible, and would be impractical to include in the calculations performed here. The empirical D value relating spin density and the ligand-centered shift should also be checked for other metalloporphyrins.

Perhaps the greatest uncertainty involved in the shift analysis results from the magnetically nonideal behavior exhibited by low-spin iron(III) complexes.[55] Deviations in Curie law behavior are apparent in Figures 2 and 3. Extrapolated intercepts (at the high-temperature limit) are generally downfield, and nonlinear plots are observed for the β-pyrrole and imidazole-5-carbon signals. Deviations appear more significant at higher temperatures. An acceptable fit for the ortho-carbon signal in the dipolar shift plot of Figure 7 is fortuitous, as choice of a temperature far removed from 26 °C for the dipolar shift analysis would yield an ortho carbon isotropic shift value decidedly noncolinear with other phenyl resonances. Nonzero Curie intercepts have previously been attributed to a significant second-order Zeeman term.[2] However, Goldammer and Zorn were unable to account for temperature dependence of the apparent coupling constant, A, by second-order Zeeman mixing in the dipolar and contact terms, and propose instead a rapid equilibrium between two configurations of Kramers doublets.[4,52] Regardless of the source, the Curie law deviations indicate the shift analysis described here is at best approximate and needs verification by appropriate calculations and other physical measurements. It should be noted again, however, that of possible axial ligands (i.e., imidazole, pyridine, cyanide ion, mercaptide ion) imidazoles appear to show the smallest second-order Zeeman deivations[22] and remain the most desirable choice for elucidating unpaired spin delocalization in low-spin iron(III) porphyrin complexes.

Magnetic complexity is also apparent in that magnetic moments for low-spin imidazole complexes are considerably higher than the expected spin-only value of 1.73 BM. A solution moment of 2.30 BM at 26 °C was obtained by the Evans' method for $[FeTPP(Im)_2]Cl$ (0.02 M FeTPPCl, 0.20 M imidazole in $CDCl_3$, 1% Me_4Si. This compares favorably with a solid-state value of 2.36 BM (4.2 to 50 K)[56] but is considerably higher than the 1.76-BM moment previously measured in solution.[9] The respective 1-methylimidazole complex exhibits a 2.3 BM moment in both solution and in the solid.[57]

Comparison with Cyanide Complexes. Differences are apparent in carbon-13 line widths observed for cyanide vs. imidazole complexes. Lines are considerably more narrow for cyanide complexes, allowing better resolution of pyrrole and meso-carbon resonances for the natural-porphyrin derivatives. This difference has been noted for proton NMR spectra of the two complexes,[11] and may result from a larger fractional population of the first excited Kramers doublet[22] and more favorable electronic relaxation in the cyanide complexes.

Comparison of FeTPP spectra also reveals considerable isotropic shift differences for certain resonances. Phenyl carbon isotropic shifts for the imidazole complexes are 2 to 4 ppm (26 °C) upfield, whereas the ortho-carbon isotropic shift for the cyanide (or cyanide/pyridine) complex is 33 ppm downfield (34 °C).[16] Signals for meta- and para-carbon atoms are shifted slightly downfield in the latter complex. Imidazole complexes exhibit a 65-ppm upfield meso-carbon shift, but the value for the cyanide complex is only 3 ppm upfield.[16] Isotropic shift values for pyrrole carbon atoms are of comparable magnitude for both complexes. Likewise, resonance positions in natural porphyrin adducts (Table VI vs. ref 17 and 20) are less sensitive to axial ligand type (when temperature differences are taken into account).

Bis-cyano iron(III) porphyrin complexes exhibit a spread of ring methyl carbon signals which is dependent on the inductive properties of 2,4-position substituents.[20] The trend is also apparent for 1-methylimidazole complexes as is indicated in Table VI for the 2,4-substituents C_2H_5, C_2H_3, H, and $COCH_3$. For the four

(54) Stock, L.M.; Wasielewski, M.R. *J. Am. Chem. Soc.* **1977**, *99*, 50–59.
(55) Kurland, R.J.; McGarvey, B.R. *J. Magn. Reson.* **1970**, *2*, 286–301.
(56) Epstein, L.M.; Straub, D.K.; Maricondi, C. *Inorg., Chem.* **1967**, *6*, 1720–1724.
(57) Hill, H.A.O.; Skyte, P.D.; Buchler, J.W.; Lueken, H.; Tonn, M.; Gregson, A.K.; Pellizer, G. *J. Chem. Soc., Chem. Commun.* **1979**, 151–152.

ring methyl signals the average deviation from the mean follows the order $C_2H_5 < C_2H_3 < H < COCH_3$, in parallel with the order of electron-withdrawing character $C_2H_5 < C_2H_3 \sim H < COCH_3$. The spread of ring methyl signals as measured by the average deviation from the mean is from 20 to 40% greater for 1-methylimidazole complexes than cyanide complexes (at the same temperature). A similar trend has been noted in the proton NMR spectra of the two types of complexes.[11] Considerable magnification in the spread of proton signals occurs for hemoproteins. This effect has been attributed to heme edge contacts,[20] the hindered rotation of an axial histidine imidazole residue,[11,52,58,59] or "strain" in the iron–imidazole linkage.[60] The possibility that preferred ring methyl proton orientation perturbs the shift pattern is not ruled out by proton NMR data alone. Observation of ring methyl carbon signals in hemoproteins will serve to clarify this point, as the spread of carbon signals should be independent of methyl group rotation.

Relation to Hemoprotein Work. Carbon-13 NMR of iron porphyrins is of obvious importance in location and assignment of prosthetic group signals of parent hemoproteins. Low sensitivity and overlap of protein resonances for the most part dictate incorporation of specific carbon-13 labels.[12] Strategy for such label insertion into the porphyrin or axial histidine group is provided by this model study. Porphyrin ring methyl labels are attractive in view of the isolated, upfield resonance positions for these groups. Label incorporation at the 2,4 positions of natural porphyrins is synthetically much more direct and should yield observable resonances. For the iron protoporphyrin prosthetic group $=CH_2$ signals are expected in the 170-ppm region and those of $=CH$ are expected in the 60-ppm region at ambient temperature. Some protein overlap is also possible for the latter residue. Likewise, for an iron(III) diacetyldeuteroporphyrin reconstituted hemoprotein in the low-spin ferric state the 2,4-carbonyl signals should be located in a "window" in the 160-ppm region.

Imidazole 2- and 4-carbon resonances are near 106 ppm, but are broadened and unlikely to be observed in a hemoprotein. The quaternary 5-imidazole carbon of histidine should remain sharp, and in fact has been tentatively assigned at 123.6 ppm (36 °C) in cyanoferricytochrome *c*.[61] Extrapolation from lower temperature measurements yields values of 114 and 111 ppm at 36 °C for the 5-carbon resonance of 5-methylimidazole (chloroform solvent) and *N*-acetylhistidine (2:1 chloroform–methanol solvent) for the FeTPP(*p*-CH_3) complexes. This difference of ~10 ppm for the protein vs. model compounds suggests effects of trans ligand or heme environment which are poorly understood, or that perhaps the tentative protein assignment should be reevaluated.

Conclusion

Imidazole-bound low-spin iron(III) porphyrins provide relevant active-site hemoprotein models, and also appear to be the magnetically most straightforward of various strong-field ligand adducts. Carbon-13 NMR spectra of both porphyrin and axial imidazole residues will be of long-term benefit in locating and assigning hemoprotein resonances, as well as in planning chemical or biological labeling experiments. Improved understanding of unpaired spin delocalization patterns constitutes a major contribution of the carbon-13 spectroscopy. Calculation of magnetic anisotropy from either proton or carbon-13 isotropic shifts reassuringly yields equivalent values, which are also approximated by ESR measurements. Detailed analysis of combined carbon and proton isotropic shift data semiquantitatively is possible for imidazole complexes as a consequence of minimal second-order Zeeman effects. Results provide estimates of unpaired spin density magnitudes at porphyrin carbon and nitrogen atoms, but should not be taken as dogmatic pending information from other physical techniques, theoretical calculations, carbon-13 relaxation measurements, and application of the carbon-13 methods described here to other metalloporphyrins.

Acknowledgement is made to the donors of the Petroleum Research Fund, administered by the American Chemical Society, for support of this research.

Supplementary Material Available: Additional tabulations (Tables S1–S13) of NMR spectra (13 pages) are available. Ordering information is given on any current masthead page.

(58) Traylor, T.G.; Berzinis, A.P. *J. Am. Chem. Soc.* **1980**, *102*, 2844–2846.
(59) Walker, F.A. *J. Am. Chem. Soc.* **1980**, *102*, 3254–3256.
(60) Goff, H. *J. Am. Chem. Soc.* **1980**, *102*, 3252–3254.
(61) Oldfield, E.; Norton, R.S.; Allerhand, A. *J. Biol. Chem.* **1975**, *250*, 6381–6402.